CHIN. PHYS. LETT. Vol. 26, No. 6 (2009) 066104

Optical Properties of Hexagonal and Cubic ZnS Nanoribbons: Experiment and Theory *

ZHANG Zhi-Hua(张志华)[1,3**], HE Ming(何明)[2], DUAN Xiao-Feng(段晓峰)[3]

[1]*Liaoning Key Materials Laboratory for Railway, Dalian Jiaotong University, Dalian 116028*
[2]*Department of physics, Dalian Jiaotong University, Dalian 116028*
[3]*Beijing National Laboratory for Condensed Matter Physics, Institute of Physics, Chinese Academy of Sciences, Beijing 100080*

(Received 5 January 2009)

Optical properties of hexagonal and cubic ZnS nanoribbons are studied by using valence electron energy loss spectroscopy (VEELS) and ab initio band structure calculations. The peaks in VEELS are assigned to interband transitions by comparing the interband transition strengths with the calculated densities of states. The optical properties are deduced from the experimental VEELS, and the theoretical calculations give consistent results. This combination of experimental and theoretical approaches provides a comprehensive understanding of the optical properties of polytype ZnS.

PACS: 61. 46. +w, 61. 72. Nn, 68. 03. Hj

Zinc sulfide (ZnS) has attracted extraordinary attention for its importance in scientific research and wide-ranging industrial, biomedical, and electronic applications.[1] Two phases, hexagonal and cubic, are observed in ZnS nanostructures. The main difference between the hexagonal wurtzite phase and cubic zinc blende phase is in the stacking orders.[2] Their total energies are very close,[3] while the two phases possess different properties.[4] The basic properties of materials, such as optical, electrical and physical behaviors, are very important to realize the applications of the polytype ZnS nanostructures. Transmission electron microscopy (TEM) and electron energy-loss spectroscopy (EELS) are appropriate techniques to investigate the optical properties of nanomaterials on account of the high spatial resolution.[5] *Ab initio* calculations, on the other hand, allow deep insight into the experimental results. In this Letter, we employ both valence electron energy loss spectroscopy (VEELS) and first-principle calculations to investigate the optical properties of hexagonal and cubic ZnS nanoribbons. The results obtained from VEELS and theoretical calculations are consistent.

The specimens studied for VEELS were ZnS nanoribbons synthesized by the thermal evaporation process.[6] A Philips CM200 field emission gun (FEG) TEM and a Tecnai F20 FEG TEM at 200 kV are used to perform the experiments. Three kinds of nanostructures appear in the studied ZnS specimens, as shown in Fig. 1(a). The selected area electron diffraction (SAED) pattern taken from specimen 1 is shown in the inset in Fig. 1(b), which can be indexed with the $[2\bar{1}\bar{1}0]_{\text{wurtzite ZnS}}$ zone axis. For specimen 2, the cubic ZnS structure with $[01\bar{1}]$ zone axis was observed in the SAED pattern (see the inset in Fig. 1(c)). The SAED pattern taken from a long strip-shaped region in the specimen 3 is shown in the inset in Fig. 1(d). Hexagonal and cubic structures are found to coexist. The orientation relations of the two phases are $[2\bar{1}\bar{1}0]||[01\bar{1}]$ and $(0001)||(111)$. The two phases coexist by sharing the same (0001) or (111) plane. Figures 1(b) and 1(c) show the high-resolution TEM (HRTEM) patterns corresponding to the specimen 1 and 2 in Fig. 1(a). The hexagonal and cubic structures are confirmed, respectively. Figure 1(d) shows the HRTEM of the strip-shaped region for specimen 3, in which hexagonal/cubic mixture structures and plane defects can be observed.

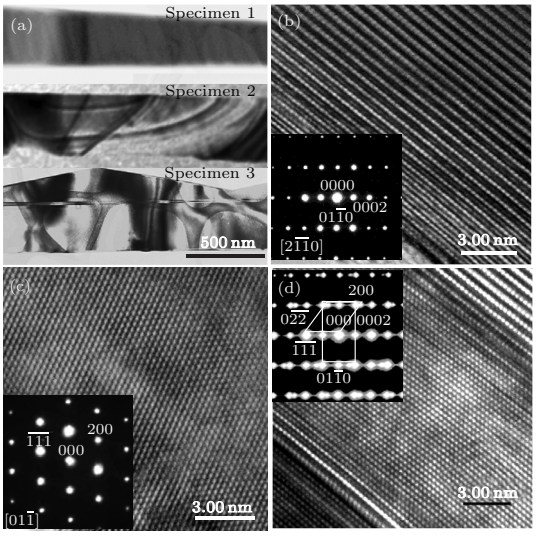


Fig. 1. (a) Low magnified TEM image of the ZnS nanoribbons. Three kinds of nanoribbons are observed, named as specimens 1, 2 and 3, respectively. HRTEM images of specimens 1 (b), 2 (c) and 3 (d), respectively. The corresponding SAED patterns are shown in the insets.

*Supported by the National Natural Science Foundation of China, and Dalian Jiaotong University.
**Email: zhzhang@djtu.edu.cn
© 2009 Chinese Physical Society and IOP Publishing Ltd

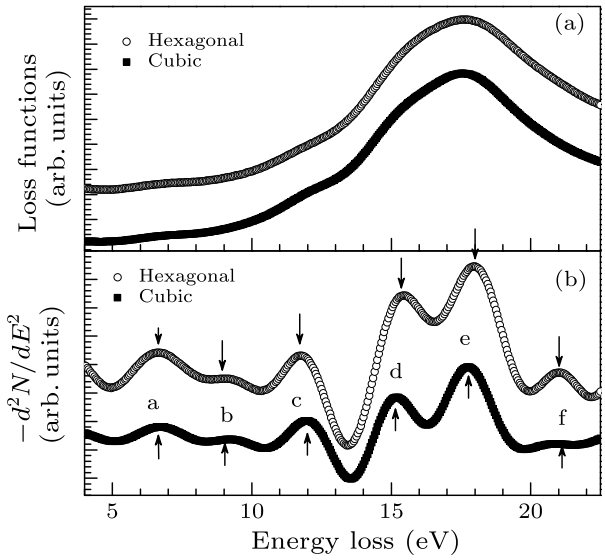


Fig. 2. (a) Loss functions to hexagonal and cubic ZnS nanoribbons, respectively. (b) The corresponding negative second-order differentiations.

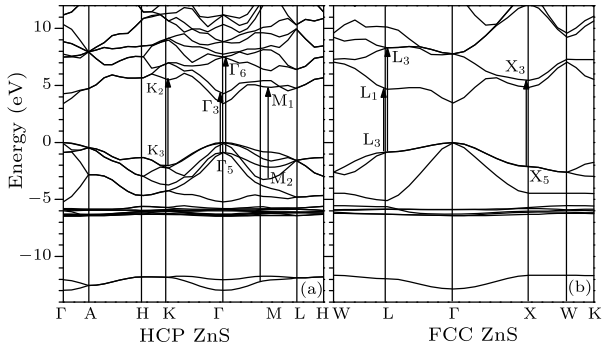


Fig. 3. Band structures of ZnS and the corresponding interband transitions (a) for hexagonal structure and (b) for cubic structure.

Our VEELS experiments were performed at zero momentum transfer with an energy resolution of about 0.75 eV. The energy dispersion was 0.05 eV/pixel and the collection semi-angle was about 2 mrad. All of the spectra were calibrated using the zero loss peak position. The typical loss functions for the hexagonal and cubic ZnS nanoribbons are shown in Fig. 2(a). To obtain the loss functions, plural scattering was first removed from the raw spectra using the conventional Fourier-log deconvolution method[7] and then the Kramers–Kronig analysis involved in the Cherenkov effects was performed.[8] The zero loss peak was removed using the method proposed by us.[9,10] Figure 2(b) shows the negative second-order differentiations of the loss functions, which gives a clearer view of the positions of the peaks. The spectra for the two phases are quite similar in their general structure. They consist of a set of low-lying shoulders at energy loss less than 10 eV (labeled as a, b), a small peak at about 11.7 eV (labeled as c), a shoulder at about 15 eV (labeled as d), a dominant peak at about 18 eV (labeled as e) and another shoulder at about 21 eV (labeled as f). The major peak e is assigned to the bulk plasma oscillation and the peak c is ascribed to the surface plasmon. The peaks a, b, d and f are associated with interband transitions.[11] The main difference between the VEELS of these two phases is the energy positions of the peaks, especially for the c, d and e peaks. The positions of plasmon peak c and e are affected by the difference of the unit cell volumes and the difference of band gap between hexagonal and cubic phases. Due to the similarity of electronic structures between the two phases (see Fig. 4), the peaks corresponding to interband transitions are located nearly at the same positions.

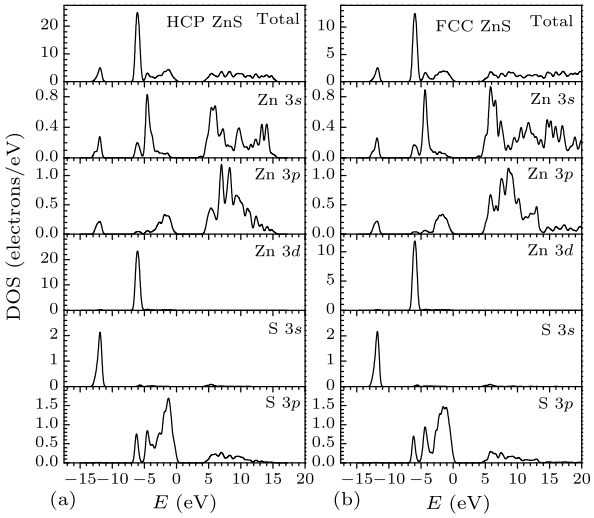


Fig. 4. DOS for hexagonal and cubic ZnS, respectively.

To determine the origins of the interband transitions, first-principle calculations were performed on the hexagonal and cubic ZnS, respectively. The ultrasoft pseudopotential was expanded within a plane wave basis set and the basis functions were truncated at the cut-off energy of 330 eV. Integrations in the Brillouin zone were performed using special K-points generated with a $6 \times 6 \times 6$ mesh parameters grid. Exchange and correlation effects were described by Perdew–Burke-Ernzerhof in the generalized gradient approximation (GGA). The calculated band gap was lower than experimental results due to the underestimation of the LDA method, so the scissors operator method was adopted and the conduction bands were shifted upward to get consistent results with the measured results. As shown in Fig. 3, the band structures are in good agreement with those in the literature.[12–15] Partial densities of state (PDOS) calculations are based on the Mulliken population analysis.[16] The results are shown in Fig. 4, from which the interband transitions corresponding to the peaks in VEELS can be derived (see Table 1). The peaks located at lower energy can also be assigned to interband transitions at symmetry points in the Brillouin zone. In comparison, the results presented in op-

tical spectrum studies [12–14] are listed in Table 1 and indexed in the energy band (Fig. 3). Because of the poor energy resolution of EELS, we observed broad structure which should be the superposition of interband transitions observed in optical spectrum studies.

Table 1. Correspondence of interband transition energies between experiment and theory. For comparison, the assignments in optical spectrum studies[12–14] to the interband transition at symmetry points in the BZ are also listed.

Transition	*hcp* ZnS(eV) assignment	*fcc* ZnS (eV) assignment
a	6.6 S 3*p*–Zn 3*s* (Γ_5 to Γ_3, M_2 to M_1 and K_3 to K_2[13,14])	
	6.6 S 3*p*–Zn 3*s* (L_3 to L_1; X_5 to X_3[12])	
b	9.3 S 3*p*–Zn 3*s* (Γ_5 to Γ_6[12])	9.3 S 3*p*–Zn 3*s* (L_3 to L_3[14])
c	11.7 surface plasmon	11.9 surface plasmon
d	15.9 Zn 3*d*–S 3*p*	15.6 Zn 3*d*–S 3*p*
e	17.8 plasmon	17.5 plasmon
f	21.0 S 3*s*–Zn 3*p*	21.0 S 3*s*–Zn 3*p*

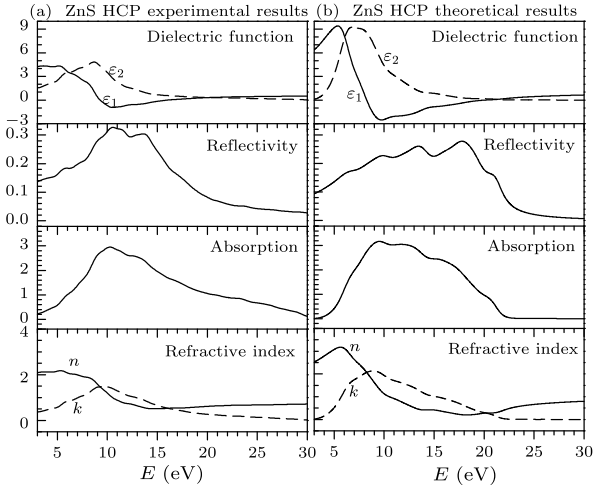


Fig. 5. Optical properties of hexagonal ZnS: (a) experimental results, (b) theoretical results.

In Figs. 5 and 6, the experimental optical properties are obtained from VEELS by the Kramers–Kronig transformation and the corresponding theoretical calculated results are shown for hexagonal and cubic ZnS, respectively. Theoretically, the smearing used is 0.7 eV and it agrees with the experimental resolution. The consistency between the experimental and theoretical results is satisfactory for both the hexagonal and cubic phases. For the complex dielectric function, ε_1 is near to unity while the value of ε_2 is very small in the high energy edge. The complex index of refraction $(n + ik)$: n is the index of refraction and k is the extinction coefficient. Reflectivity R can be measured by vacuum ultraviolet (VUV) spectroscopy directly. Compared with other techniques, EELS significantly extends the energy range and is a useful technique for analysis of the dielectric properties on a microstructural level. Our results give some references to the thorough understanding of the optical properties of ZnS.

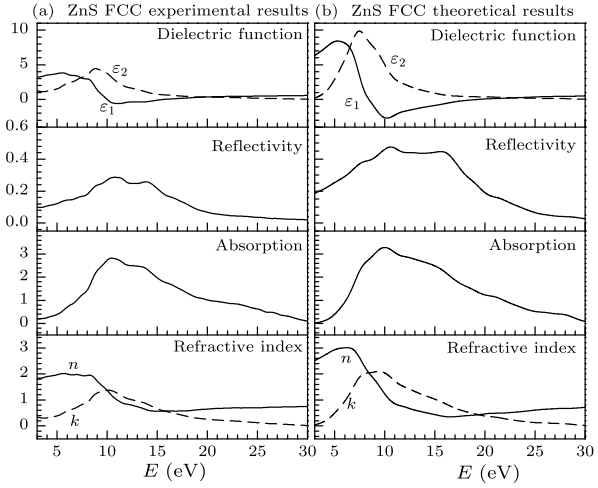


Fig. 6. Optical properties of cubic ZnS: (a) experimental results, (b) theoretical results.

In conclusion, the electronic structure and optical properties of hexagonal and cubic ZnS nanoribbons have been investigated by VEELS and first principle calculations systematically. The peaks appearing in VEELS are assigned to interband transitions and the symmetry points of the Brillouin zone. The optical properties are obtained from experimental VEELS and *ab initio* calculations, which give consistent results. The combining of experimental and theoretical approaches gives a comprehensive understanding of the optical properties of polytype ZnS.

We thank Professor Quan Li for help.

References

[1] Ma C, Moore D, Li J and Wang Z L 2003 *Adv. Mater.* **15** 228
[2] Birman J L 1959 *Phys. Rev.* **115** 1493
[3] Engel G E and Needs R J 1990 *J. Phys.: Condens. Matter* **2** 367
[4] Brafman O and Mitra S S 1968 *Phys. Rev.* **171** 931
[5] Arenal R, Stéphan O, Kociak M, Taverna D, Loiseau A and Colliex C 2005 *Phys. Rev. Lett.* **95** 127601
[6] Wang F F, Zhang Z H, Liu R B, Wang X, Zhu X, Pan A L and Zou B S 2007 *Nanotechnology* **18** 305705
[7] Egerton R F 1986 *Electron Energy Loss Spectroscopy in the Electron Microscope* (New York: Plenum)
[8] Stoeger-Pollach M and Schattschneider P 2007 *Ultromicrioscopy* **107** 1178
[9] Zhang Zhi-Hua, Qi X Y, Jian J K and Duan Xiao Feng 2006 *Micron* **37** 229
[10] Zhang Zhi-Hua, Yang J J, He Ming and Li Quan 2008 *Appl. Phys. Lett.* **92** 171903
[11] Hengehold R L and Pedrotti F L 1972 *Phys. Rev.* **6** 3026
[12] Bergstresser T K and Cohen M L 1967 *Phys. Rev.* **164** 1069
[13] Cardona M and Harbeke G 1964 *Phys. Rev.* **137** A1467
[14] Stukel D J, Euwema R N, Collins T C, Herman F and Kortum R L 1968 *Phys. Rev.* **179** 740
[15] Rössler U 1969 *Phys. Rev.* **184** 733
[16] Segall M D, Pickard C J, Shah R and Payne M C 1996 *Mol. Phys.* **89** 571